

On the Spine of a PDE Surface

Hassan Ugail

Department of Electronic Imaging and Media Communications
School of Informatics, University of Bradford
Bradford BD7 1DP, UK
h.ugail@bradford.ac.uk

Abstract. The spine of an object is an entity that can characterise the object's topology and describes the object by a lower dimension. It has an intuitive appeal for supporting geometric modelling operations. The aim of this paper is to show how a spine for a PDE surface can be generated. For the purpose of the work presented here an analytic solution form for the chosen PDE is utilised. It is shown that the spine of the PDE surface is then computed as a by-product of this analytic solution.

This paper also discusses how the of a PDE surface can be used to manipulate the shape. The solution technique adopted here caters for periodic surfaces with general boundary conditions allowing the possibility of the spine based shape manipulation for a wide variety of free-form PDE surface shapes.

1 Introduction

Generally speaking the spine of an object is the trace of the center of all spheres (disks in the case of two dimensions) that are maximally inscribed in the object [6]. The spine of an object has a very close geometric resemblance to the more widely known shape entity called the medial axis or the skeleton [9]. Bearing in mind the general definition for a spine, one could therefore imagine that the spine of a shape brings out the symmetries in that shape. It can also be noted that the spine in general has far richer topologies than the shape it is derived from. Other important properties of the spine of a shape include its use in the intermediate representation of the object and its canonical general form that can be used to represent the object by a lower dimensional description.

Apart from the rich geometric properties the spine posses, many have also noted its intuitive appeal in applications in geometric manipulations. For example Blum [6] suggested the spine or the skeleton as a powerful mechanism for representing the shape of two dimensional objects at a level higher than cell-enumeration. He proposed a technique that can uniquely decompose a shape into a collection of sub-objects that can be readily identified with a set of basic primitive shapes. Many others have affirmed the flexibility of the spine and its ability to naturally capture important shape characteristics of an object [12,11,7].

Despite its intuitive appeal the spine is rarely used in CAD systems for supporting geometric modelling operations. Among the reasons for this include the

lack of robust implementations of spine generating procedures for existing CAD techniques, and the inability to demonstrate the wide range of shape manipulations that can be potentially performed using the spine of a shape.

In spite of this a number of methods for constructing the spine of polyhedral models as well as free-form shapes have been proposed. These include topological thinning [13], Euclidian distance transform [1] and the use of deformable snakes [10]. The majority of the existing techniques use numerical schemes to scan the domain of the whole object in order to generate its spine. Thus, these algorithms not only consume excessive CPU time to perform their operations but also are prone to errors.

The focus of this paper is on the spine of the PDE surfaces. PDE surfaces are generated as solutions to elliptic Partial Differential Equations (PDEs) where the problem of surface generation is treated as a boundary-value problem with boundary conditions imposed around the edge of the surface patch [2,3,16]. PDE surfaces have emerged as a powerful shape modelling technique [8,14,15]. It has been demonstrated how a designer sitting in front of a workstation is able to create and manipulate complex geometry interactively in real time [14]. Furthermore, it has been shown that complex geometry can be efficiently parameterised both for intuitive shape manipulation [15] and for design optimisation [5].

The aim of this paper is to show how the spine of a PDE surface can be created and utilised in order to characterise PDE surfaces as well as to enable the development of further intuitive techniques for powerful shape manipulations. By exploiting the structural form of a closed form solution for the chosen PDE, it is shown how the spine of a PDE surface can be generated as a by-product of this solution. Furthermore, it is shown that the spine of the PDE surface patch is represented as a cubic polynomial that can be used as a shape manipulation tool to deform the shape in an intuitive fashion. It is also shown that, by exploiting a general form of an analytic solution method, the spine for PDE surfaces with general boundary conditions can equally be represented as a by-product of the solution that generates the surface shape. To demonstrate the ideas presented here, practical examples of shapes involving PDE surfaces are discussed throughout the paper.

2 PDE Surfaces

A PDE surface is a parametric surface patch $\underline{X}(u, v)$, defined as a function of two parameters u and v on a finite domain $\Omega \subset R^2$, by specifying boundary data around the edge region of $\partial\Omega$. Typically the boundary data are specified in the form of $\underline{X}(u, v)$ and a number of its derivatives on $\partial\Omega$. Moreover, this approach regards the coordinates of point u and v as a mapping from that point in Ω to a point in the physical space. To satisfy these requirements the surface $\underline{X}(u, v)$ is regarded as a solution of a PDE of the form,

$$D_{u,v}^m \underline{X}(u, v) = \underline{F}(u, v), \quad (1)$$

where $D_{u,v}^m \underline{X}(u, v)$ is a partial differential operator of order m in the independent variables u and v , while $\underline{F}(u, v)$ is a vector valued function of u and v . Since

boundary-value problems are of concern here, it is natural to choose $D_{u,v}^m \underline{X}(u, v)$ to be elliptic.

Various elliptic PDEs could be used, although the most widely used PDE is based on the biharmonic equation namely,

$$\left(\frac{\partial^2}{\partial u^2} + a^2 \frac{\partial^2}{\partial v^2} \right)^2 \underline{X}(u, v) = 0. \tag{2}$$

Here the boundary conditions on the function $\underline{X}(u, v)$ and its normal derivatives $\frac{\partial \underline{X}}{\partial n}$ are imposed at the edges of the surface patch.

With this formulations one can see that the elliptic partial differential operator in Equation (2) represents a smoothing process in which the value of the function at any point on the surface is, in some sense, a weighted average of the surrounding values. In this way a surface is obtained as a smooth transition between the chosen set of boundary conditions. The parameter a is a special design parameter which controls the relative smoothing of the surface in the u and v directions [3].

2.1 Solution of the PDE

There exist many methods to determine the solution of Equation (2). In some cases, where the boundary conditions can be expressed as relatively simple analytic functions of u and v , it is possible to find a closed form solution. However, for a general set of boundary conditions a numerical method often need to be employed.

For the work on the spine to be described here, restricting to periodic boundary conditions the closed form analytic solution of Equation (2) is utilised. Choosing the parametric region to be $0 \leq u \leq 1$ and $0 \leq v \leq 2\pi$, the periodic boundary conditions can be expressed as,

$$\underline{X}(0, v) = \underline{p}_0(v), \tag{3}$$

$$\underline{X}(1, v) = \underline{p}_1(v), \tag{4}$$

$$\underline{X}_u(0, v) = \underline{d}_0(v), \tag{5}$$

$$\underline{X}_u(1, v) = \underline{d}_1(v). \tag{6}$$

Note that the boundary conditions $\underline{p}_0(v)$ and $\underline{p}_1(v)$ define the edges of the surface patch at $u = 0$ and $u = 1$ respectively. Using the method of separation of variables, the analytic solution of Equation (2) can be written as,

$$\underline{X}(u, v) = \underline{A}_0(u) + \sum_{n=1}^{\infty} [\underline{A}_n(u) \cos(nv) + \underline{B}_n(u) \sin(nv)], \tag{7}$$

where

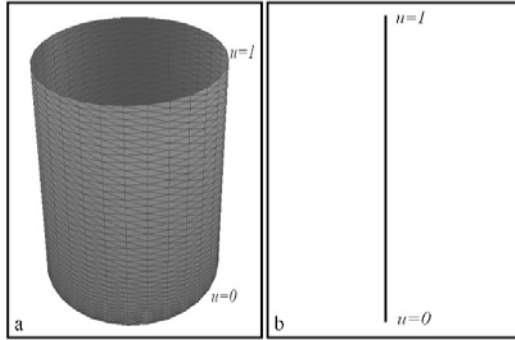


Fig. 1. Description of the spine of a PDE surface. (a) A ‘cylindrical’ PDE surface. (b) The spine described by the \underline{A}_0 term.

$$\underline{A}_0 = \underline{a}_{00} + \underline{a}_{01}u + \underline{a}_{02}u^2 + \underline{a}_{03}u^3, \tag{8}$$

$$\underline{A}_n = \underline{a}_{n1}e^{anu} + \underline{a}_{n2}e^{anu} + \underline{a}_{n3}e^{-anu} + \underline{a}_{n4}e^{-anu}, \tag{9}$$

$$\underline{B}_n = \underline{b}_{n1}e^{anu} + \underline{b}_{n2}e^{anu} + \underline{b}_{n3}e^{-anu} + \underline{b}_{n4}e^{-anu}, \tag{10}$$

where $\underline{a}_{00}, \underline{a}_{01}, \underline{a}_{02}, \underline{a}_{03}, \underline{a}_{n1}, \underline{a}_{n2}, \underline{a}_{n3}, \underline{a}_{n4}, \underline{b}_{n1}, \underline{b}_{n2}, \underline{b}_{n3}$ and \underline{b}_{n4} are vector-valued constants, whose values are determined by the imposed boundary conditions at $u = 0$ and $u = 1$.

3 The Spine of a PDE Surface

Taking the form of Equation (7) one could observe the following properties of the analytic solution that allows us to extract the spine of a PDE surface as a by-product of the solution. Firstly the term \underline{A}_0 in Equation (7) is a cubic polynomial of the parameter u . Secondly it can be seen that for each point $\underline{X}(u, v)$ on the surfaces the term $\sum_{n=1}^{\infty} [\underline{A}_n(u) \cos(nv) + \underline{B}_n(u) \sin(nv)]$ in Equation (7) describes the ‘radial’ position of the point $\underline{X}(u, v)$ relative to a point at \underline{A}_0 .

Thus, the term \underline{A}_0 which is a cubic polynomial of the parameter u and lies within the periodic surface patch. Therefore, using the solution technique described in Equation (7) a surface point $\underline{X}(u, v)$ may be regarded as being composed of sum of a vector \underline{A}_0 giving the position on the spine of the surface and a radius vector defined by the term $\sum_{n=1}^{\infty} [\underline{A}_n(u) \cos(nv) + \underline{B}_n(u) \sin(nv)]$ providing the position of $\underline{X}(u, v)$ relative to the spine. What follows in the rest of this section describes some examples of PDE surfaces and the corresponding spines relating to the \underline{A}_0 term given in Equation (7).

Fig. 1(a) shows a typical PDE surface where the boundary conditions are taken as,

$$\underline{p}_0(v) = (0.5 \cos v, 0.5 \sin v, 0), \tag{11}$$

$$\underline{p}_1(v) = (0.5 \cos v, 0.5 \sin v, 0.5), \tag{12}$$

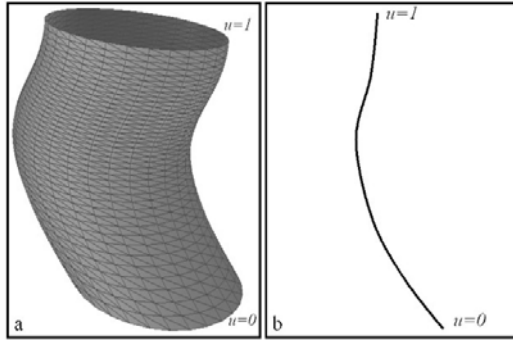


Fig. 2. Description of the spine of a PDE surface. (a) A deformed ‘cylindrical’ PDE surface. (b) The spine described by the \underline{A}_0 term.

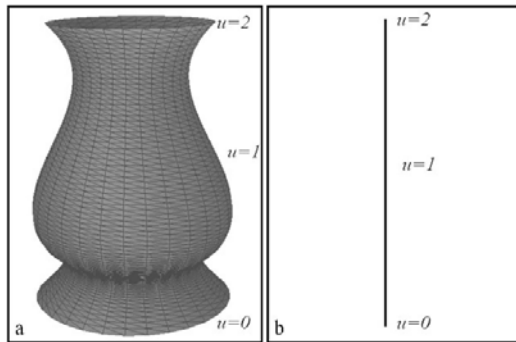


Fig. 3. Description of the spine of a composite PDE surface. (a) A composite PDE surface describing a vase shape. (b) The spine of the vase shape.

$$\underline{d}_0(v) = (0.5 \cos v, 0.5 \sin v, 1), \tag{13}$$

$$\underline{d}_1(v) = (0.5 \cos v, 0.5 \sin v, 1). \tag{14}$$

Fig. 1(b) shows the image of the cubic polynomial described by the \underline{A}_0 term corresponding to the spine for this surface patch.

Fig. 2(a) shows another example of a single PDE patch where the boundary conditions were taken to be that described by the previous example with the exception that the circle defining $\underline{d}_1(v)$ was translated by an amount of 0.2 units along the negative x-axis. The resulting spine for this surface patch is shown in Fig. 2(b). As can be noted in both these examples the spine closely describes the midline or the skeleton of the surfaces patch.

Fig. 3(a) shows a composite shape that looks like the shape of a vase. This shape is created by means of two surface patches with a common boundary at $u = 1$. Again the boundary conditions for these surface patches are circular and similar to those used to create Fig. 1(a). Furthermore, for the two surface patches the derivative conditions at $u = 1$ were taken in such a way to ensure

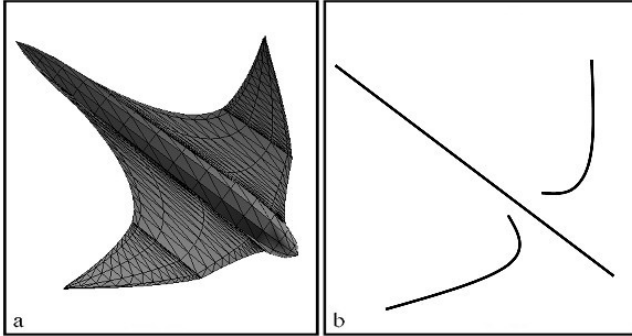


Fig. 4. Aircraft created using a composite of 5 PDE surface patches. (a) The aircraft shape. (b) The corresponding composite spine.

that tangent plane continuity between them is maintained. The corresponding spine for the vase shape is shown is Fig. 3(b).

Fig. 4(a) shows a composite shape that looks like the shape of an aircraft. This shape is created by means of four surface patches. The corresponding composite spine for the aircraft shape is shown is Fig. 4(b).

4 Shape Manipulation Using the Spine

One of the many attractive features of the PDE surfaces is the ability to be able to create and manipulate complex shapes with ease. Previous work on interactive design has demonstrated that the user having little or no knowledge about solving PDEs and how the boundary conditions effect the solutions of the PDEs is able to use the method to create complex geometry with ease [14,15].

The aim of this section is to show that the spine of a PDE surface can be utilised to create design tools for further efficient shape manipulation. As shown in the previous section the spine of a PDE surface comes as a by-product of the analytic solution used. By virtue of the very definition of the spine it can be seen as a powerful and intuitive mechanism to manipulate the shape of surface once it is defined. There are many ways by which one could utilise the spine to manipulate a PDE surface. One such possibility is described here.

We can express the cubic polynomial described by \underline{A}_0 in Equation (7) to be a Hermite curve of the form,

$$\underline{H}(u) = \underline{B}_1(u)\underline{p}_0 + \underline{B}_2(u)\underline{p}_1 + \underline{B}_3(u)\underline{v}_0 + \underline{B}_4(u)\underline{v}_1, \tag{15}$$

where the \underline{B}_i are the Hermite basis functions, $\underline{p}_0, \underline{p}_1$ and $\underline{v}_0, \underline{v}_1$ define the position and the speed of the Hermite curve at $u = 0$ and $u = 1$ respectively. By comparing the Hermite curve given in Equation (15) with the cubic for the spine given by the \underline{A}_0 term in Equation (7), the terms $\underline{a}_{00}, \underline{a}_{01}, \underline{a}_{02}$ and \underline{a}_{03} described in Equation (8) can be related to the position vectors and its derivatives at the end points of the spine as,

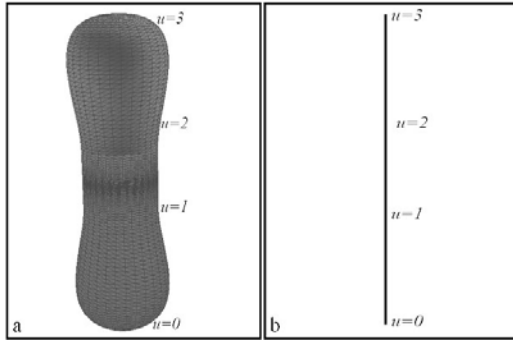


Fig. 5. PDE vesicle shape. (a) The vesicle shape created using three surface patches. (b) The spine of the vesicle shape.

Table 1. Vector values for the position vectors and its derivatives at the end of points of the spine for the vesicle shapes shown in Figs. 5 and 6.

vector	Fig. 5 (x, y, z)	Fig. 6 (x, y, z)
\underline{p}_0	(0.0, -1.0, 0.0)	(0.1, -1.0, 0.0)
\underline{p}_1	(0.0, 1.0, 0.0)	(0.4, 1.0, 0.0)
\underline{v}_0	(0.0, -0.2, 0.0)	(-0.1, 0.1, 0.0)
\underline{v}_1	(0.0, 0.2, 0.0)	(-0.3, -0.2, 0.0)

$$\underline{a}_{00} = \underline{p}_0, \tag{16}$$

$$\underline{a}_{01} = 3\underline{p}_1 - \underline{v}_1 - 3\underline{v}_0, \tag{17}$$

$$\underline{a}_{02} = \underline{v}_1 + 2\underline{v}_0 - 2\underline{p}_1, \tag{18}$$

$$\underline{a}_{02} = \underline{v}_0. \tag{19}$$

Since the \underline{A}_0 term in Equation (7) is an integral part of the solution that generates the surface shape, any change in the shape of the spine will of course results in a change in the shape of the surface. A useful mechanism to change the shape of the spine would be to manipulate its position and the derivative at the two end points. Therefore, the position vectors and its derivatives at the end of points of the spine can be used as shape parameter to manipulate the shape.

To demonstrate this idea consider the vesicle shape, similar to that of a human red blood cell, shown in Fig. 5(a) where the corresponding spine is also shown in 5(b). The vesicle shape is created using three surface patches with common boundaries between the adjacent patches at $u = 1$ and $u = 2$. The boundary conditions for this problem are circles similar to those used in the example shown in Fig. 1, with the positional boundary conditions at $u = 0$ and $u = 3$ taken to be points in 3-space.

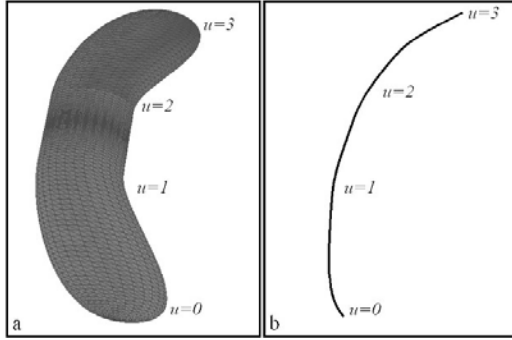


Fig. 6. New PDE vesicle shape. (a) The vesicle shape created by manipulating the spine. (b) The manipulated spine of the new vesicle shape.

The vesicle can be then manipulated by making changes to the shape of the spine via the vectors $\underline{p}_0, \underline{p}_1, \underline{v}_0$ and \underline{v}_1 . Table 1 shows the value for the x, y and z components of the vectors $\underline{p}_0, \underline{p}_1, \underline{v}_0$ and \underline{v}_1 for the vesicle shown in Fig. 5(a) and those for the manipulated shape shown in Fig. 6(a). Fig. 6(b) shows the manipulated spine. Note that throughout this shape manipulation process the derivative conditions at $u = 1$ and $u = 2$ were taken in a manner to ensure tangent plane continuity between the adjacent surface patches is maintained. This also ensures that the corresponding spine has tangent continuity at $u = 1$ and $u = 2$.

In previous work discussed in [5], involving the problem of determining the shapes of the stable structures occurring in human red blood cells, a similar vesicle structure as shown in Fig. 5 was used as a starting shape of an optimisation processes. These shapes were parameterised using the appropriate Fourier coefficients, where some of the intermediate shapes resulted during the optimisation process resembled the shape of the vesicle shown in Fig. 6. An interesting and rather intuitive way to parameterise the vesicle geometry would be the spine approach outlined here.

5 General PDE Boundary Conditions and the Spine

One could note that the examples described above are somewhat simple where the shapes are generated using simple boundary conditions possessing analytic forms. However, to cater for a wide range of possible free-form shape manipulations the spine of shapes with general boundary conditions need to be addressed. For this purpose the approach adopted here is to use a previously developed solution technique which can handle general periodic boundary conditions [4]. The method is based on a spectral approximation providing an approximate analytic solution form of the chosen PDE. The basic idea behind this solution method is presented here with details on how the solution affects the spine. For detailed discussions of this solution method the interested reader is referred to [4].

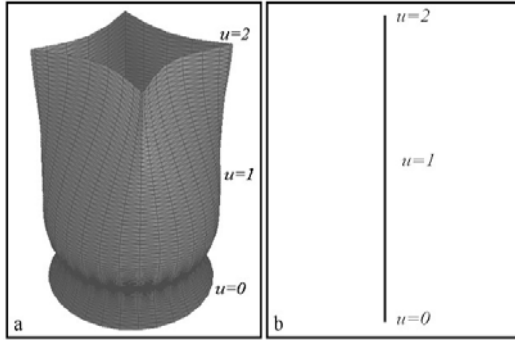


Fig. 7. Description of the spine of a PDE surface with general boundary conditions. (a) A vase shape with general boundary conditions at $u = 2$ defined as cubic B-spline curves. (b) The spine of the vase shape.

For a general set of boundary conditions, in order to define the various constants in the solution, it is necessary to Fourier analyse the boundary conditions and identify the various Fourier coefficients. Where the boundary conditions can be expressed exactly in terms of a finite Fourier series, the solution given in Equation (7) will also be finite. However, this is often not possible, in which case the solution will be the infinite series given Equation (7).

The technique for finding an approximation to $\underline{X}(u, v)$ is based on the sum of the first few Fourier modes and a ‘remainder term’, i.e.,

$$\underline{X}(u, v) \simeq \underline{A}_0(u) + \sum_{n=1}^N [\underline{A}_n(u) \cos(nv) + \underline{B}_n(u) \sin(nv)] + \underline{R}(u, v), \quad (20)$$

where usually $N \leq 6$ and $\underline{R}(u, v)$ is a remainder function defined as,

$$\underline{R}(u, v) = \underline{r}_1(v)e^{wu} + \underline{r}_2(v)e^{wu} + \underline{r}_3(v)e^{-wu} + \underline{r}_4(v)e^{-wu}, \quad (21)$$

where $\underline{r}_1, \underline{r}_2, \underline{r}_3, \underline{r}_4$ and w are obtained by considering the difference between the original boundary conditions and the boundary conditions satisfied by the function,

$$\underline{F}(u, v) = \underline{A}_0(u) + \sum_{n=1}^N [\underline{A}_n(u) \cos(nv) + \underline{B}_n(u) \sin(nv)]. \quad (22)$$

An important point to note here is that although the solution is approximate this new solution technique guarantees that the chosen boundary conditions are exactly satisfied since the remainder function $\underline{R}(u, v)$ is calculated by means of the difference between the original boundary conditions and the boundary conditions satisfied by the function $\underline{F}(u, v)$.

It is noteworthy that the introduction of the $R(u, v)$ term in the new solution described in Equation (20) has virtually no effect in the interior shape of the

surfaces. This is because, for large enough n , the Fourier modes make negligible contributions to the interior of the patch. Therefore, by taking a reasonable truncation of the Fourier series at some finite N , (say $N = 6$) of the boundary conditions an approximate PDE surface can be quickly generated satisfying the boundary conditions exactly. Furthermore, as far as the spine is concerned since the spine does not represent the detailed geometry of the shape the $\underline{A}_0(u)$ term is left unchanged in the approximate solution and hence the spine of the shape is left unchanged. Fig. 7 exemplifies this.

Fig. 7(a) shows a vase shape similar to that shown in Fig. 3(a), where the position and derivative boundary conditions at $u = 2$ were taken as periodic cubic B-spline curves with cusps. The curves along with the rest of the boundary conditions which are in analytic form were used in the solution outlined to create the shape shown in Fig. 7(a). The corresponding spine for the new vase shape is shown in Fig. 7(b).

6 Conclusions

This paper describes how the spine of a PDE surfaces can be generated. Due to the analytic form of the solution used to generate the surface shape the spine is computed as a by-product of the solution. This outlines the advantage of using PDE surfaces for modelling since in the case of most other techniques for shape generation the spine has to be computed separately.

Due to the canonical and intuitive nature of the spine it can be used to manipulate the shape once the shape is defined. It has been demonstrated how simple shape manipulation can be carried out using the spine of a PDE surface. The solution technique adopted here caters periodic surfaces with general boundary conditions with the spine derived as a by-product of the solution. This allows the possibility of the spine based shape manipulation for a wide variety of free-form surface shapes.

As shown here the shape manipulation using the spine can be seen as an added bonus to the existing intuitive tools available for efficient shape manipulation of PDE surfaces. An interesting future direction of study would be to parameterise the shapes based on the spine described here. This would allow one to create geometry that can handle not only complex shapes but also shapes with changing topology. Such a parameterisation scheme then can be applied to design optimisation problems where a wide variety of geometry with changing topology would be available to the optimisation scheme.

References

1. Arcelli, C., and Sanniti di Baja, G.: Ridge Points in Euclidean Distance Maps. *Pattern Recognition Letters*, **13**(4) (1992) 237-243
2. Bloor, M. I. G., and Wilson, M. J.: Generating Blend Surfaces Using Partial Differential Equations, *Computer-Aided Design*. **21** (1989) 165-171
3. Bloor, M. I. G., and Wilson, M. J.: Using Partial Differential Equations to Generate Freeform Surfaces. *Computer Aided Design*, **22** (1990) 202-212

4. Bloor, M.I.G., and Wilson, M.J.: Spectral Approximations to PDE Surfaces. *Computer-Aided Design*, **28** (1996) 145–152
5. Bloor, M. I. G. and Wilson, M. J.: Method for Efficient Shape Parametrization of Fluid Membranes and Vesicles. *Physical Review E*, **61**(4) (2000) 4218–4229
6. Blum, H.: A transformation for Extracting New Descriptors of Shape. In: Wathen-Dunn, W. (ed.): *Models for Perception of Speech and Visual Form*, MIT Press (1976) 362-381
7. Boissonnat, J. D.: Geometric Surfaces for 3-Dimensional Shape Representation. *ACM Transactions on Graphics*, **3**(4) (1984) 244-265
8. Du, H., and Qin, H.; Direct Manipulation and Interactive Sculpting of PDE Surfaces. *Computer Graphics Forum (Proceedings of Eurographics 2000)*, **19**(3) (2000) 261-270
9. Dutta, D and Hoffmann, C.M.: On the Skeleton of Simple CSG Objects. *ASME Journal of Mechanical Design*, **115**(1) (1992) 87-94
10. Leymarie, F., and Levine, M.D.: *Skeleton from Snakes*, Progress in Image Analysis and Processing, World Scientific Singapore (1990)
11. Nackman, L.R., and Pizer, S.M.: Three-Dimensional Shape Description using Symmetric Axis Transform. *IEEE Transactions on Pattern Analysis and Machine Intelligence*, **7**(2) (1985) 187-202
12. Patrikalakis, N.M., and Gursoy, H.N.: Shape Interrogation by Medial Axis Transform. In: Ravani, B. (ed.): *Advances in Design Automation: Computer-Aided Computational Design*, ASME **1** (1990) 77-88
13. Tsao, Y.F., and Fu, K.S.: A Parallel Thinning Algorithm for 3-D Pictures. *Computer Graphics Image Process*, **17** (1981) 315-331
14. Ugail, H., Bloor, M.I.G., and Wilson, M.J.: Techniques for Interactive Design Using the PDE Method. *ACM Transactions on Graphics*, **18**(2) (1999) 195–212
15. Ugail, H., Bloor, M.I.G., and Wilson, M.J.: Manipulations of PDE Surfaces Using an Interactively Defined Parameterisation. *Computers and Graphics*, **24**(3) (1999) 525–534
16. Vida, J., Martin, R.R., and Varady, T.: A Survey of Blending Methods that use Parametric Surfaces. *Computer-Aided Design*, **26**(5) (1994) 341–365